

# 國科會專題研究結案報告

波導結構光電元件及相關介觀材料結構研究 -

子計畫一：新型半導體及非線性光電元件

**Novel Semiconductor and Nonlinear Optics Devices**

計畫主持人：楊志忠 執行單位：國立台灣大學光電所

計畫編號：NSC 89-2218-E-002-095

執行期限：89年8月1日至90年10月31日

## 中文摘要

我們利用在週期性區域反轉鋁酸鋰上的非共線相位匹配條件下的光參作用，達成了於紅外線區段內 300 毫微米頻寬的訊號波及 635 毫微米頻寬的閑置波。

## 英文摘要

Experimental demonstration of broadband generation on PPLN based on noncollinear phase matching optical parametric process is reported. Bandwidths of 300 nm for signal and 635 nm for idler in the near infrared range were achieved.

## 1. Introduction

Broadband optical sources have applications in many areas, such as WDM signal generation and amplification of fiber communications, optical coherence tomography, and spectroscopy of large excitation tunability. In this paper, we report the experimental implementation of broadband optical parametric generation in PPLN based on a novel phase-matching retracing behavior. The retracing behavior was implemented with non-collinear pumping of a PPLN optical parametric process. Although non-collinear pumping of QPM nonlinear processes was reported [9-11], retracing behaviors for broadband generation like our results have not been discussed in the literature. Here, we show the experimental and theoretical results of broadband optical parametric generation (OPG) in PPLN, pumped with a Q-switched Nd:YAG laser. The signal wavelength can be as broad as 300 nm with the central wavelength ranging from 1.66 through 1.96  $\mu\text{m}$ .

## 2. Theoretical Predictions

Figure 1 shows the non-collinear phase-matching geometry. An angle  $\theta$  is defined between the pump beam direction and the

normal to the QPM grating inside PPLN. The angle between pump and signal beams is  $\delta$  and the angle between pump and idler beams is  $\gamma$ . The angle  $\alpha$  represents the incident angle of the pump in air. Here,  $K_p$ ,  $K_s$ ,  $K_i$ , and  $K_g$  represent the magnitudes of wavevectors of the pump ( $K_p$ ), signal ( $K_s$ ), idler ( $K_i$ ), and QPM grating ( $K_g$ ), respectively. Here, the signal is defined to have a wavelength shorter than that of the idler. Fig. 2(a) shows the theoretical predictions of the phase-matching condition for OPG. The signal wavelength is shown as a function of pump angle  $\theta$  based on a 29.5- $\mu\text{m}$  period PPLN with temperature varied from 160  $^{\circ}\text{C}$  to 200  $^{\circ}\text{C}$ . Here, we assume that the idler propagates along the normal to the QPM structure ( $\gamma = \theta$ ). The pump wavelength is 1.064  $\mu\text{m}$ . Retracing behavior of phase-matching angle can be clearly seen when the signal wavelength is near 1.8  $\mu\text{m}$ . Such a retracing behavior can result in broadband generation. Based on our calculations, similar phenomena can be observed with other pump wavelengths and periods of PPLN. Figure 2(b) shows the retracing behaviors of phase-matching angle  $\theta$  with a PPLN period around 24  $\mu\text{m}$  when the pump wavelength is 900 nm and temperature is fixed at 179  $^{\circ}\text{C}$ . Here, it is assumed that the signal propagates along the normal to the QPM structure. We can see that the phase-matching curve becomes almost vertical near  $\theta = 1.252^{\circ}$  when the PPLN period is 24.3  $\mu\text{m}$ . We predicate that with appropriate experimental conditions, a broadband source ranging from 1.42 through 1.65  $\mu\text{m}$  is feasible.

## 3. Experimental Setup

In our experiment, a Q-switched Nd:YAG laser (Coherent, Infinity 40-100) with pulse width 3.5 ns was used for pumping. A lens system was employed to focus the pump beam into a waist of 190  $\mu\text{m}$  (diameter) inside a PPLN crystal. The 1.9-cm long PPLN crystal contained

eight different QPM-period structures. Each structure is 1.3 mm in width and about 0.1 mm separated from the neighboring structures. The pump beam coverage of other QPM periods is small. The crystal was placed in an oven, whose temperature can be varied up to 250 °C with accuracy 0.1 °C.

#### 4. Experimental Results

Figure 3 shows four signal spectra of different pump angles with 29.5- $\mu\text{m}$  period PPLN and temperature fixed at 190 °C. When the PPLN crystal was rotated to increase  $\alpha$  (and hence  $\theta$ ), the central wavelength ( $\lambda_{sc}$ ) and full-width-at-half-maximum (FWHM) spectral width ( $\Delta\lambda_s$ ) of signal spectra varied from  $\lambda_{sc} = 1.563 \mu\text{m}$  with  $\Delta\lambda_s = 8.5 \text{ nm}$  (curve I -- collinear case) to the broadest case of  $\lambda_{sc} = 1.81 \mu\text{m}$  with  $\Delta\lambda_s = 300 \text{ nm}$  (curve III -- from 1.66  $\mu\text{m}$  to 1.96  $\mu\text{m}$  at  $\alpha = 4^\circ$ , the corresponding  $\theta$  is 1.85°). Because of water vapor absorption near 2  $\mu\text{m}$  and bandwidth limitation of our spectrum analyzer, the broadest signal spectrum is non-symmetric. With further increase of  $\theta$  to 2.3°, FWHM spectral width was reduced to 140 nm (curve IV -- centered at 1.84  $\mu\text{m}$ ). In the case of the broadest signal spectral width, the corresponding bandwidth of idler is 635 nm near 2.5  $\mu\text{m}$ . In these experiments, the pumping threshold for observing the broadband outputs based on our detection facilities increased from 0.334 to 1.25 mJ as  $\theta$  varied from 0 to 2.3°. Such threshold increase is mainly due to the decreasing beam overlap as  $\theta$  increases.

These results are summarized in Fig. 4. Here, various dashed curves represent theoretical predictions of different phase-matching conditions (from right to left:  $\gamma = \theta$ ,  $\gamma = 1.1\theta$ ,  $\gamma = 1.2\theta$ , and  $\gamma = 1.3\theta$ ). The symbols stand for the signal spectral peak position and the vertical bars show the corresponding FWHM spectral ranges. The experimental results are quite consistent with the theoretical predictions, particularly when  $\theta$  is small. When  $\theta$  becomes large, the experimental results differ somewhat from predictions. This difference is due to our assumption in theoretical calculation that the idler propagates in the direction normal to the QPM grating. When  $\gamma$  is large, since there is no cavity to confine the idler propagation direction, it may propagate in other directions. Hence, the experimental bandwidth is broader than what predicted. Note that different signal and idler

output wavelength components propagate in different directions. Such angle chirp may lead to difficulty in collecting broadband outputs. However, it represents an advantage in WDM communication application.

The insert of Fig. 4 shows the temperature dependence of signal wavelength with  $\alpha = 4^\circ$ . The PPLN period is now 29.7  $\mu\text{m}$ . One can see that the acceptance temperature range for broadband generation can be several centigrade. However, temperature variation leads to the change of conversion efficiency. In our experiments, we also observed efficient sum-frequency generation (SFG) from the mixing of pump and signals in certain directions between  $K_p$  and  $K_s$ . Based on our calculations, the SFG was due to the interaction of non-collinear configuration with the third-order QPM.

Similar to Fig. 4, Fig. 5 shows the results when OPG was pumped with an elliptical laser beam of 100  $\mu\text{m}$  x 900  $\mu\text{m}$ . The larger beam width was along the PPLN crystal surface. The PPLN period was 29.7  $\mu\text{m}$ . Compared to the case of a circular pump beam, the output bandwidths of the elliptical pump beam are smaller. This is so because the focused circular beam has a broader variation of pump wavevector, leading to broader phase-matching conditions and hence broader output bandwidths. In this experiment, pump threshold increased from 0.751 mJ for the collinear case to 1.15 mJ for  $\theta = 1.85^\circ$ .

#### 5. Conclusions

In summary, with non-collinear OPG on PPLN, we have theoretically predicted retracing behaviors of phase matching and experimentally demonstrated the generation of broadband signal and idler beams. The broadest signal spectrum covered the wavelength range from 1.66 through 1.96  $\mu\text{m}$ . The corresponding idler wavelength ranged from 2.328 through 2.963  $\mu\text{m}$ . Note that the OPG output bandwidth reported can be reduced if an OPO is implemented because of the propagation direction confinement of either signal or idler. Such reduction will not much affect broadband generation if the case of Fig. 2(b) is considered.

#### References:

1. S. T. Yang and S. P. Velsko, Opt. Lett. 24, 133 (1999).

2. M. J. Missey, V. Dominic, P. E. Powers and K. L. Schepler, *Opt. Lett.* 24, 1227 (1999).
3. V. Smilgevicius, A. Stabinis, A. Piskarskas, V. Pasiskevicius, J. Hellstrom, S. Wang, and F. Laurell, *Opt. Comm.* 365 (2000).

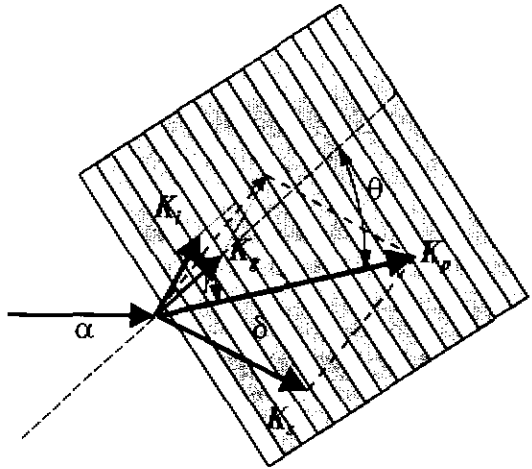


Fig. 1 Configuration of non-collinear phase matching.

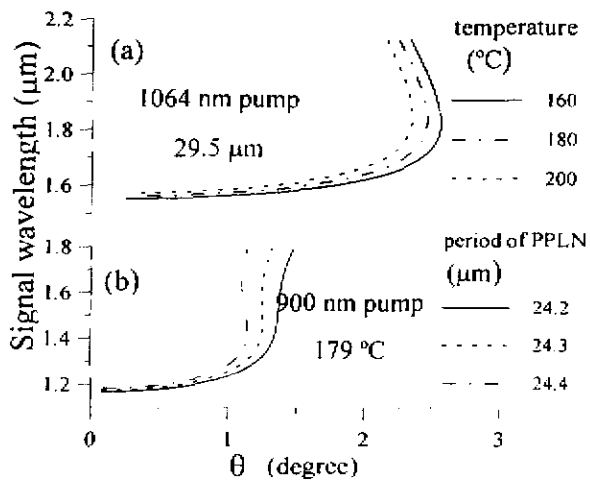


Fig. 2 Theoretical angle tuning curves with various PPLN periods and pump wavelengths.

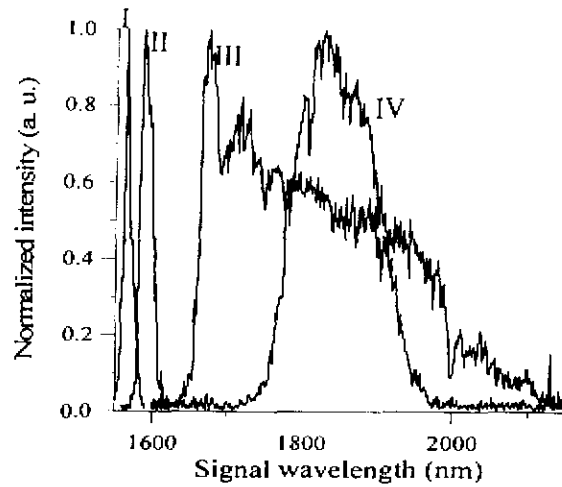


Fig. 3 Output signal spectra for several  $\theta$  angles.

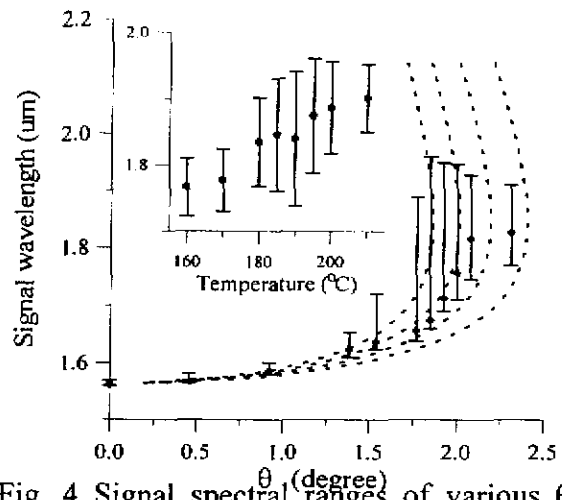


Fig. 4 Signal spectral ranges of various  $\theta$  angles.

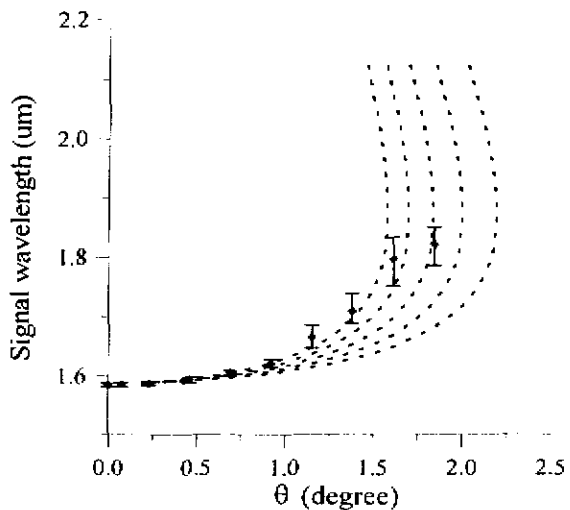


Fig. 5 Similar to Fig. 4 except that the crystal is pumped with an elliptical beam of  $100 \mu\text{m} \times 1 \text{mm}$ .

## 出國開會報告

會議名稱：歐洲雷射與光電研討會

European Conference on Lasers and Electro-Optics (CLEO/EUROPE)

日期：西元 2000 年 9 月 10 日至 9 月 15 日

地點：法國尼斯 (Nice)

此次歐洲雷射與光電研討會選擇在旅遊聖地，臨地中海的尼斯舉行，的確吸引了不少參加者，參加人數約為 1500 人。此次 CLEO/EUROPE 乃是他們最後一次在西元偶數年辦理此會，下一次將跳至西元 2003 年九月辦理。由於我國將於西元 2003 年七月辦理亞太地區類似之研討會，為避免爭取參加者之競爭，本人特別與其相關人員協調會議之重點，避免重複。歐洲會議仍然承續其研究工作長處，在固態雷射與生醫光電上多所發揮，然而，因光纖通訊崛起，相關系統與元件也受到重視。